

## Hydration structures in proteins and neutron diffraction experiment on dissimilatory sulfite reductase D (DsrD)

Toshiyuki Chatake,<sup>a</sup> Andreas Ostermann,<sup>a</sup> Kazuo Kurihara,<sup>a</sup> Fritz G. Parak,<sup>b</sup> Nobuhiro Mizuno,<sup>c</sup> Gerrit Voordouw,<sup>d</sup> Yoshiki Higuchi,<sup>e</sup> Ichiro Tanaka<sup>a</sup> and Nobuo Niimura<sup>a,f,\*</sup>

<sup>a</sup>Neutron Structural Biology, Neutron Science Research Center, Japan Atomic Energy Research Institute, Tokai, Ibaraki, 319-1195, Japan, <sup>b</sup>Physik Department E17, TU Munchen, James-Frank-Str., 85748, Germany, <sup>c</sup>Division of Chemistry, Graduate School of Science, Kyoto University, Sakyo, Kyoto 606-8502, Japan, <sup>d</sup>Department of Biological Sciences, the University of Calgary, Alberta, T2N 1N4, Canada, <sup>e</sup>Department of Life Science, Graduate School and Faculty of Science, Himeji Institute of Technology, Koto, Kamigori, Ako-gun, Hyogo 678-1297, Japan, and <sup>f</sup>Faculty of Technology, Ibaraki University, Hitachi, Ibaraki, 316-8511, Japan. E-mail: niimura@kotai3.tokai.jaeri.go.jp

Neutron crystallography can provide a substantial amount of information about the hydration of proteins. The hydration patterns of three proteins, whose structures have been solved at 1.5 or 1.6 Å resolution using our BIX-type diffractometers, show interesting features. The water molecules adopt a variety of shapes in the neutron Fourier maps, revealing details of intermolecular hydrogen-bond formation and dynamics of hydration. In addition, the neutron diffraction study of a DNA-binding protein, dissimilatory sulfite reductase D (DsrD) is briefly described, and some preliminary results are presented. This topic is of interest because it is well-known that hydrogen bonds play important roles in DNA-protein recognition.

### 1. Introduction

Water molecules surrounding water-soluble proteins are suspected to mediate some biological processes via the formation of hydrogen-bonds (H-bonds). For a full understanding of the finer structural details, it is necessary to know the orientations of the hydrogen atoms (or deuterium atoms) in the water molecules. In past investigations, neutron crystallographers have observed various shapes of water molecules in neutron Fourier maps (Habash *et al.*, 2000, Shu *et al.*, 2000, Bon *et al.*, 1999, Niimura *et al.*, 1997, Kossiakoff *et al.*, 1992, Schoenborn, 1988, Harrison *et al.*, 1988); however, recently we have been able to extend these studies to a higher level of resolution (1.5 or 1.6 Å). We have carried out the neutron structure analyses of these proteins, sperm whale myoglobin, a wild-type rubredoxin from *Pyrococcus furiosus*, and a mutant of the latter protein using the neutron diffractometer BIX-3 at JAERI (Tanaka *et al.*, 2002). Their hydration structures including the positions of H atoms have been observed, and the intrinsic shapes of the hydration peaks could be seen in real detail from these higher resolution analyses (Chatake *et al.*, 2003).

A topic of even greater potential interest items from the well-known fact that a DNA binding protein interacts with the nucleic acid by a combination of direct H-bonds and water-mediated H-bonds, in order to achieve specific and precise DNA-protein recognition. Currently, we are trying to determine the neutron crystal structure of dissimilatory sulfite reductase D (DsrD), a protein which contains a B-DNA or Z-DNA binding motif (Mizuno *et al.*, 2002, 2003). In view of the

fact that a crystal larger than 1 mm<sup>3</sup> is necessary for neutron analysis, we found it useful to develop a method for systematically growing large crystals. In this manuscript, we describe how we found the right conditions for crystal growth, using a two-pronged approach: a combination of a 'crystallization phase diagram' combined with 'crystal quality assessment' via preliminary X-ray searching.

### 2. Hydration of proteins

#### 2.1. Hydration patterns observed in neutron Fourier maps

Fig. 1 shows one region of the hydration structure around myoglobin. The scattering length of hydrogen atoms are negative and the density contours in neutron Fourier maps are written in red, while deuterium, carbon, nitrogen and oxygen atoms have positive neutron scattering lengths, and they appear as blue contours. Hydrogen (deuterium<sup>†</sup>) atoms in the water molecules can be clearly identified in this figure as triangular-shaped contours and the formation of certain H-bonds between the water molecules and the protein can be recognized as well. Moreover, other types of water molecules, such as ellipsoidal and spherical peaks, have been found in other places, and the classification of water molecule contours and their nature will be the major topic of discussion in this article.

We have categorized the observed water molecules into the following classes based on their appearance in Fourier maps: (i) triangular, (ii) ellipsoidal, and (iii) spherical shape. Moreover, in the second category, the ellipsoidal stick shapes are further classified as (iia) short and (iib) long. We have found that this classification conveniently reflects the degree of order and the dynamic behavior of a water molecule. A typical example of (i) the triangular shape is shown in Fig. 2(a), in which the blue and green contours indicate  $2|F_o| - |F_c|$  maps calculated from neutron and X-ray data, respectively. The oxygen positions observed

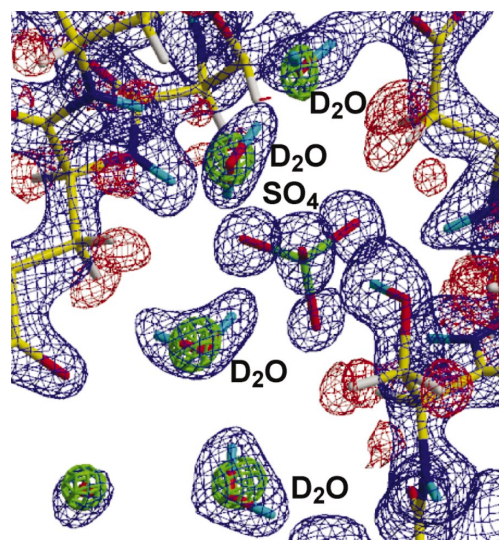


**Figure 1**

Protein-protein contact region in the case of myoglobin.  $2|F_o| - |F_c|$  neutron density map contoured at 1.5 sigma in blue and -2.0 sigma in red. The  $2|F_o| - |F_c|$  X-ray map for the water molecules is shown in green (The contour of each water molecule is in a range of 2.0 sigma - 3.5 sigma). The triangular shaped neutron contours correspond to D<sub>2</sub>O molecules.

<sup>†</sup> In neutron diffraction experiments, protein are generally crystallized from, or soaked in D<sub>2</sub>O solutions in order to avoid the very strong incoherent neutron scattering from H atoms (<sup>1</sup>H) which gives rise to undesirably high background counts. In this report, the term water molecule means D<sub>2</sub>O, not H<sub>2</sub>O.

by X-ray and neutron scattering coincide within experimental error. In Fig. 2(a), the two D atoms and the O atom of the water molecule are H-bonded to the atoms of the nearest oxygen and/or nitrogen atoms (O/N atoms) and a deuterium atom, respectively. Thus, it can be seen that the orientation of this water molecule is well-defined. In fact, the triangular-shaped contours correspond to the most highly-ordered water molecules in our maps. A typical example of (iia), a short ellipsoidal peak, is shown in Fig. 2(b). The oxygen position observed by X-rays is located at the end of the neutron Fourier peak, but only one deuterium atom could be observed. The observed D and O atoms are H-bonded to neighboring O/N and D atoms respectively, but the other deuterium atom was not identified because of the molecular rotation (or packing disorder) around the fixed O-D bond. Thus, we interpret short ellipsoidal peaks to represent water molecules rotationally disordered around their O-D bonds. A typical example of the (iib), a long ellipsoidal peak, is shown in Fig. 2(c). The O position, which was observed by X-rays is located in the middle of the neutron Fourier peak and the two D atoms are only seen in part. The entire appearance is that of a stick, or an elongated ellipsoid. Although the two D atoms are H-bonded to neighboring O or N atoms, their complete scattering density cannot be seen because of the molecular rotation or packing disorder around the axis parallel to the D-D axis. A typical example of (iii) the spherical shaped peak is shown in Fig. 2(d). Only the center of gravity of this type of water molecule can be defined because its orientation is totally disordered. It should be kept in mind that the boundaries (between the four different classifications of water molecules) are not sharp.

## 2.2. H-bonds in hydration and shell structure

We found that the observed shapes of the water molecules are strongly correlated with the number of hydrogen bonds they make. In Fig. 3, the distribution of the number of anchor points<sup>‡</sup> (not the number of H-bonds) for the water molecules of the three proteins are shown. This diagram shows that the most of the triangular shaped water molecules are fixed at three atoms (D, O, D), while ellipsoidal ones are mostly fixed at two atoms (D, D or D, O).

It would have been interesting to see if there is any correlation between the shape of a water molecule and its location in hydration shells (i.e., its distance from the surface of a protein). We have found that, on the surface of a protein, all types of water molecules can be found. However, triangular shaped water molecules are either connected directly to the surface through H-bonds, or indirectly through other triangular shaped peaks. The populations of triangular, ellipsoidal and spherical shapes between the first and the second shells are largely different. This tendency coincides with the result of a neutron crystallographic analysis of crambin (Teeter & Kossiakoff, 1984), in which it was noticed that water molecules become increasing disordered as one moves further away from the surface of a protein.

## 2.3. Dynamic behavior of water molecules

The dynamic behavior of water molecules can be appreciated when the B-factors obtained by neutron and X-ray are plotted against each other as shown in Fig. 4. The B-factors of oxygen atoms obtained by X-rays are in the range from 13 Å<sup>2</sup> to 45 Å<sup>2</sup>. It is seen that, in general, the small, intermediate and large B-factors from the X-ray analysis

<sup>‡</sup> Note: the number of anchor points refers to the number of atoms involved in hydrogen bonding, and this number is not always equal to be the number of H-bonds made by that water molecule. For example, in solid ice each water molecule makes four H-bonds, but the number of anchor points in that case is only three.

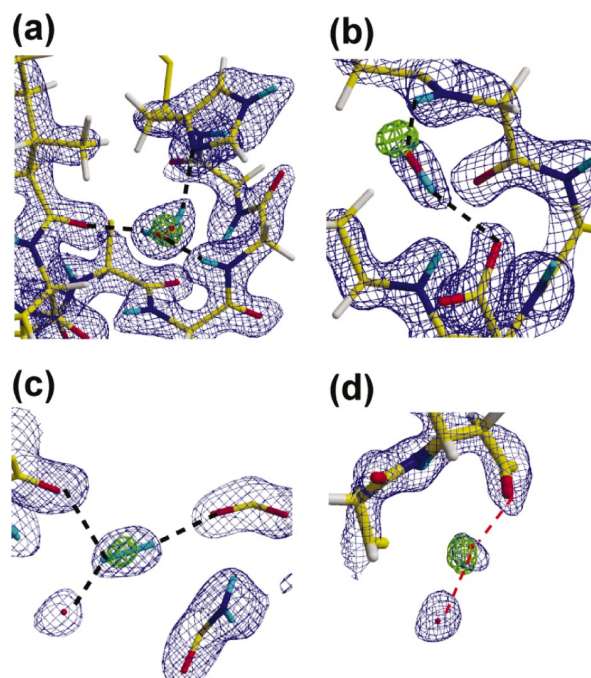


**Figure 2**  
2|*F*<sub>o</sub>|-|*F*<sub>c</sub>| maps of water molecules of hydration for myoglobin and a rubredoxin mutant observed by neutron protein crystallography. Examples shown are those of: (a) triangular shape, (b) short ellipsoidal shape, (c) long ellipsoidal shape and (d) spherical shape. In these maps, the blue contours correspond to neutron peaks, while the green contours correspond to oxygen peaks from X-ray data. Observed atoms from the neutron data are shown as stick diagrams.

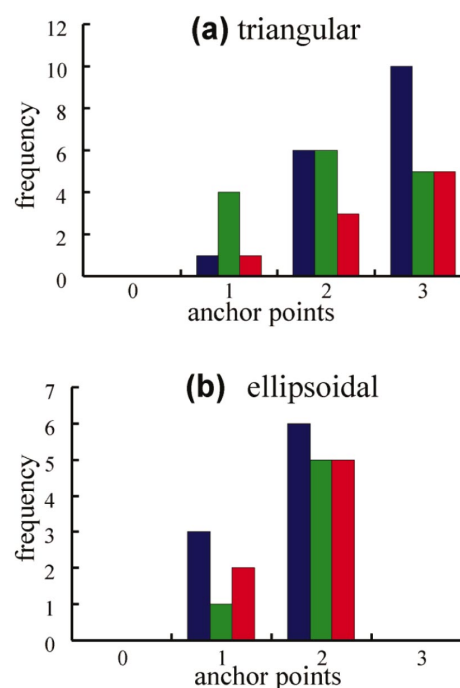


**Figure 3**  
Number of anchor points for water molecules having (a) triangular shape and (b) ellipsoidal shape. One anchor point means that one atom of a D<sub>2</sub>O molecule is fixed with one or more hydrogen bonds of the type O(N)-D — Y, in which the D atom is clearly observed. Hydrogen bonds X-H — Y were included in this diagram if the D — Y distance is less than 2.8 Å, and if the X-H — Y angle is more than 90 degree. The blue, green and red bars show the numbers for myoglobin, rubredoxin-wild and rubredoxin-mutant, respectively.

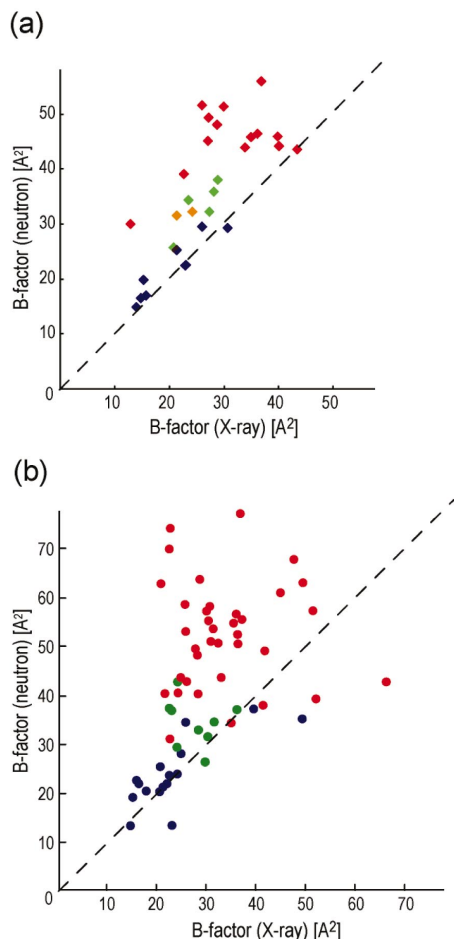


**Figure 4**  
Correlation between the B-factors of hydration water molecules obtained from neutron and X-ray scattering data for (a) the rubredoxin mutant and (b) myoglobin. The squares are colored by their own shapes. Blue, green, orange and red squares correspond to triangular, short ellipsoidal, long ellipsoidal and spherical peaks in neutron Fourier maps, respectively. Note that low B values correspond to well-ordered water molecules (triangle peaks), while high B values correspond to disordered water molecules (spherical peaks).

correspond to water molecules having the triangular, ellipsoidal and spherical shapes in the neutron analysis, respectively.

In summary, we have shown that the four major classifications of water molecules, (i) triangular, (iia) short ellipsoids, (iib) long ellipsoids and (iii) spherical-shaped peaks, correspond to D<sub>2</sub>O molecules with increasing disorder. Hydration networks connecting O atoms have been previously observed in numerous X-ray studies of proteins, but in our case (because we can also see the H/D atoms in our neutron studies) we can provide more details through the shapes of the contours described in this article, in contrast to X-ray studies which only provide the oxygen positions. Earlier neutron studies have shown some variation in the shapes of water molecules in neutron Fourier maps, but the low resolutions of these studies significantly limited any detailed analysis of their shapes. In the present study, the resolutions of our structure analyses are much higher (1.5 ~ 1.6 Å), allowing almost all of the contour shapes of the water molecules in Fourier maps to be completely isolated, and making it easy to classify the water molecules. Moreover we could correlate the shapes of water molecules with the number of anchored atoms, and also correlate these shapes with their dynamic behavior (i.e., with their B-factors). Finally, we should point out that the detailed water structure observed by high-resolution neutron protein crystallography provides not only

information about where a water molecule is located, but also how it binds to the neighboring atoms.

### 3. Neutron diffraction experiment of dissimilatory sulfite reductase D (DsrD)

#### 3.1. Crystallization of the DsrD protein

DsrD was produced and purified as already reported (Hittel & Voordouw, 2000). Before crystallization, DsrD was dialyzed against D<sub>2</sub>O solution for 2 days and incubated for 4 months. The purpose of this H/D exchange step is to reduce high background noise caused by the incoherent scattering of hydrogen atoms in the neutron experiment. As mentioned earlier, it was necessary to devise a systematic way of growing large crystals of this protein for the neutron experiment, and we started by first growing crystals for preliminary X-ray screening trials. Fig. 5 shows the crystallization phase diagram of DsrD in the vapor diffusion system. Six crystals (shown as numbers in Fig. 5) were used for an initial quality analysis using X-ray diffraction. X-ray diffraction images were collected by the oscillation method. Total rotation angle of each data set was planned to cover more than 90% independent reflections. A maximum resolution criterion (of the X-ray diffraction pattern) and an overall B-factor were used for the comparison between the crystals. Fig. 5 shows that crystal #2 had the highest resolution (1.8 Å) diffraction pattern and the lowest B-factor (13.8 Å<sup>2</sup>) of the six crystals that were tested. Consequently, further crystallization experiments were focused on the initial conditions that produced crystal #2. After that, a macro-seeding technique was used to obtain a large crystal with these optimum crystallization conditions. This large crystal (1.7mm<sup>3</sup>) was obtained after four successive seeding experiments. From our results, it can be concluded that the use of (1) 'a crystallization phase diagram' (Fig. 5) coupled with (2) 'crystal-quality assessment techniques' (using maximum resolutions and overall B-factor of crystals as criteria) were useful techniques in

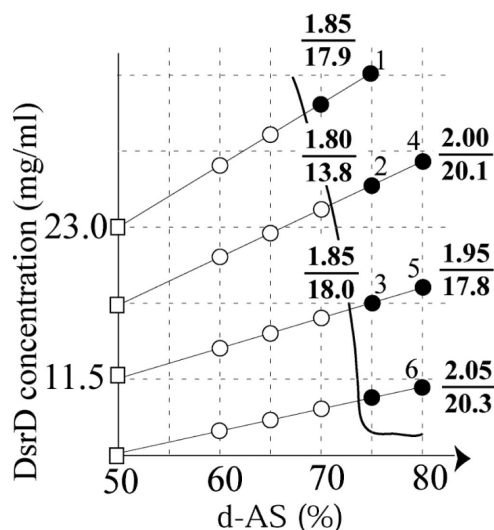


**Figure 5**  
The crystallization phase diagram of DsrD in vapor diffusion system. A curve means the nucleation curve. The vertical axis is the protein concentration, and the horizontal axis is the deuterated ammonium sulfate concentration. The squares show the initial conditions of the crystallization solutions, while the circles show the equilibrated conditions. The numbers correspond to the crystals produced in this experiment, which were subsequently used for quality analysis by X-ray diffraction. The results of the assessment of the crystal quality are shown as fractional numbers. In each case, the numerator indicates the maximum resolution, while the denominator indicates the overall B-factor.

carrying out the task of growing large crystals. A more detailed description of the crystallization experiments will be reported elsewhere.

### 3.2. Neutron diffraction experiment of DsrD

The neutron diffraction experiment was carried out at room temperature using a monochromatic neutron beam ( $\lambda = 2.88 \text{ \AA}$ ) with the BIX-3 diffractometer, located at reactor JRR-3M of JAERI (Tanaka et al., 2002). The crystal of DsrD belongs to the space group of  $P2_12_12_1$ , with cell dimensions of  $a = 60.5 \text{ \AA}$ ,  $b = 65.1 \text{ \AA}$ ,  $c = 46.5 \text{ \AA}$ . Neutron diffraction images were collected using the step-scan method with an interval of 0.3 degree. The total time for the data collection was 70 days. The diffraction patterns were integrated with the programs DENZO and SCALEPACK (Otwinowski & Minor, 1997), and merged up to a maximum resolution of  $2.4 \text{ \AA}$  with an overall  $R_{\text{merge}}$  value of 0.143. The completeness of the data was 0.925 (0.821 in the highest shell,  $2.49 \sim 2.40 \text{ \AA}$ ). The structure determination was performed by the molecular replacement method, using the X-ray crystal structure of DsrD as the initial model. Before least-squares refinement, the D atoms of the main polypeptide chain, and H atoms whose positions could be estimated stereochemically, were added to the model. After the first cycles of refinement with the program CNS (Brunger et al., 1998), the R-factor was 0.287 ( $R_{\text{free}} = 0.308$ ). A portion of the H-bonding network was observed in the neutron  $2|\text{Fo}| - |\text{Fc}|$  Fourier map on the surface of the protein, illustrating a system of direct H-bonds and a series of water-mediated H-bonds linking the polar residues Lys40, Tyr63 and Thr44. The structure analysis of this protein is continuing, and full results will be reported in the future.

We thank to Professor Robert Bau for valuable suggestions and an assistance in refining the expression of this manuscript. This study is

carried out as a part of a 'Development of New Structural Biology Including Hydrogen and Hydration' project, funded by the Organized Research Combination System (ORCS), and promoted by the Ministry of Education, Culture, Sports, Science and Technology of Japan.

### References

- Bon, C., Lehmann, M.S. & Wilkinson, C. (1999). *Acta Crystallogr.* textbfD55, 978–987.
- Brünger, A. T., Adams, P. D., Clore, G. M., DeLano, W. L., Gros, P., Grosse-Kunstleve, R. W., Jiang, J. S., Kuszewski, J., Nilges, N., Pannu, N. S., Read, R. J., Rice, L. M., Simonson, T., Warren, G. L. (1998). *Acta Cryst.* **D54**, 905–921.
- Chatake, T., Ostermann, A., Kurihara, K., Parak, F.G. & Niimura, N. (2003). *Proteins*, **50**, 516–523.
- Habash, J., Raftery, J., Nuttall, R., Price, H.J., Wilkinson, C., Kalb, A.J. & Helliwell, J.R. (2000). *Acta Crystallogr.* **D56**, 541–550.
- Harrison, R.W., Woldawer, A. & Sjolín, L. (1988). *Acta Crystallogr.* **A44**, 309–320.
- Hittel, D. S. & Voordouw, G. (2000). *Antonie van Leeuwenhoek; J. Microbiol. Serol.* **77**, 13–22.
- Kossiakoff, A.A., Sintchak, M.D., Shpungin, J. & Presta, L.G. (1992). *Proteins* **12**, 223–236.
- Mizuno, N., Voordouw, G., Miki, K., Sarai, A. & Higuchi, Y. (2003). *Structure*, to be published.
- Mizuno, N., Hittel, D. S., Voordouw, G. & Higuchi, Y. (2002). *Acta Cryst.* **A58** (Supplement), C304.
- Niimura, N., Minezaki, Y., Nonaka, T., Castagna, J.C., Cipriani, F., Hoghoj, P., Lehmann, M.S. & Wilkinson, C. (1997). *Nat. Struct. Biol.* **4**, 909–914.
- Otwinowski, Z. & Minor, W. (1997). *Methods Enzymol.* **276**, 307–326.
- Schoenborn B.P. (1988). *J. Mol. Biol.* **201**, 741–749.
- Shu, F., Ramakrishnan, V. & Schoenborn, B.P. (2000). *Proc. Natl. Acad. Sci. USA* **97**, 3872–3877.
- Tanaka, I., Kurihara, K., Chatake, T. & Niimura, N. (2002). *J. Appl. Cryst.* **35**, 34–40.
- Teeter, M.M. & Kossiakoff, A.A. (1984). *Basic life science* **27**. New York and London: Plenum Press, p335–348.